

# Organometallic complexes for nonlinear optics. Part 27. Syntheses and optical properties of some iron, ruthenium and osmium alkynyl complexes<sup>☆</sup>

Clem E. Powell<sup>a</sup>, Marie P. Cifuentes<sup>a</sup>, Andrew M. McDonagh<sup>a</sup>,  
Stephanie K. Hurst<sup>a</sup>, Nigel T. Lucas<sup>a</sup>, Christopher D. Delfs<sup>a</sup>, Robert Stranger<sup>a</sup>,  
Mark G. Humphrey<sup>a,\*</sup>, Stephan Houbrechts<sup>b</sup>, Inge Asselberghs<sup>b</sup>, André Persoons<sup>b</sup>,  
David C.R. Hockless<sup>c</sup>

<sup>a</sup> Department of Chemistry, Australian National University, Canberra, ACT 0200, Australia

<sup>b</sup> Laboratory for Chemical and Biological Dynamics, University of Leuven, Celestijnenlaan 200D, B-3001 Leuven, Belgium

<sup>c</sup> Research School of Chemistry, Australian National University, Canberra, ACT 0200, Australia

Received 27 September 2001; accepted 30 October 2001

Dedicated to Professor Martin Bennett in recognition of his outstanding contributions to organometallic chemistry

## Abstract

The syntheses of the alkynyl complexes  $M(4-C\equiv CC_6H_4NO_2)(dppe)(\eta-C_5H_5)$  [ $M = Fe$  (**1**),  $Ru$  (**2**),  $Os$  (**3**)],  $Os(4-C\equiv CC_6H_4NO_2)(PPh_3)_2(\eta-C_5H_5)$  (**4**) and  $Ru(4-C\equiv CC_6H_4NO_2)(CO)_2(\eta-C_5H_5)$  (**5**) are reported. Structural studies reveal a decrease in  $Ru-C(1)$  distance on proceeding from **5** to **2**, consistent with greater back-donation of electron density to the alkynyl ligand from the more electron-rich metal center in **2**. Electrochemical data show that the  $M^{II/III}$  couple for the dicarbonyl complex **5** is at a significantly more positive potential than that of the related diphosphine complex **2**, consistent with ligand variation modifying the electron richness and hence donor strength of the metal center. Time-dependent density functional calculations on model complexes  $M(4-C\equiv CC_6H_4NO_2)(PH_3)_2(\eta-C_5H_5)$  ( $M = Fe, Ru, Os$ ) have been employed to assign the intense low-energy optical transition in these complexes as MLCT in character, the higher energy band being phenyl–phenyl\* in nature. Molecular quadratic optical nonlinearities have been measured using the hyper-Rayleigh scattering procedure at 1064 nm.  $\beta$  values vary as  $Fe \leq Ru \leq Os$  for metal variation and  $CO <$  phosphines for co-ligand variation, the latter consistent with the variation in donor strength of the metal center inferred from electrochemical and crystallographic data. The observed trend in  $\beta$  on metal variation follows the trend in backbonding energies calculated by DFT.

© 2003 Elsevier Science B.V. All rights reserved.

**Keywords:** Iron; Ruthenium; Osmium; Cyclic voltammetry; X-ray structure; Alkynyl; NLO; Density functional theory

## 1. Introduction

The nonlinear optical (NLO) properties of organometallic complexes have attracted significant attention over the past decade [2–6]. The vast majority of organometallics for which NLO properties have been

investigated have the donor–bridge–acceptor composition which has been shown to afford organic materials with high NLO merit. In this complex composition, the ligated metal can adopt the donor, bridge, or acceptor role, and for some bimetallics the metal can function as both donor and acceptor. A plethora of studies have focussed on modification of the organic bridging ligands, and many studies have assessed the effect of variation of the co-ligands at the ligated metal center on optical nonlinearity. One less-explored area which is of fundamental importance for the utility of organometallics in NLO applications is the effect of metal variation

<sup>☆</sup> Part 26: see Ref. [1].

\* Corresponding author. Tel.: +61-2-6125 2927; fax: +61-2-6125 0760.

E-mail address: [mark.humphrey@anu.edu.au](mailto:mark.humphrey@anu.edu.au) (M.G. Humphrey).

on nonlinearity. Group 8 metal variation in metallocenyl [7–10] and nitrile [11] complexes revealed the quadratic NLO efficiency series  $\text{Fe} > \text{Ru}$ , suggesting a correlation with ease of oxidation; for the nitrile complexes, correlation with  $\nu(\text{C}\equiv\text{N})$  values was found, suggestive of the importance of backbonding [11]. We have previously examined analogous 14 valence electron gold alkynyl complexes and 18 valence electron nickel alkynyl complexes, noting an increase in  $\beta$  values on increasing metal valence electron count [12,13], and 18 valence electron ruthenium complexes, observing a further increase in  $\beta$  values which may result from increasing ease of oxidation [14,15]. We report herein synthesis of a systematically varied series of 4-nitrophenylalkynyl complexes of the Group 8 metals, examination of their spectroscopic data, electrochemical properties and selected crystallographic data, their molecular quadratic nonlinearities at 1064 nm, and approximate density functional calculations which have been undertaken in order to understand the electronic structure and optical properties, and rationalize the observed trend in optical nonlinearities.

## 2. Experimental

### 2.1. General remarks

Reactions were carried out using Schlenk techniques under an atmosphere of nitrogen, although subsequent work up was carried out without any precautions to exclude air. The following were prepared by literature methods: 4- $\text{HC}\equiv\text{CC}_6\text{H}_4\text{NO}_2$  [16],  $\text{RuCl}(\text{CO})_2(\eta\text{-C}_5\text{H}_5)$  [17],  $\text{FeCl}(\text{dppe})(\eta\text{-C}_5\text{H}_5)$  [18],  $\text{RuCl}(\text{dppe})(\eta\text{-C}_5\text{H}_5)$  [19],  $\text{OsBr}(\text{dppe})(\eta\text{-C}_5\text{H}_5)$  [19], and  $\text{Fe}(4\text{-C}\equiv\text{CC}_6\text{H}_4\text{NO}_2)(\text{CO})_2(\eta\text{-C}_5\text{H}_5)$  (**6**) [20]. The literature procedure for the preparation of  $\text{OsBr}(\text{PPh}_3)_2(\eta\text{-C}_5\text{H}_5)$  [21] was modified in the following way: MeOH was substituted for EtOH as solvent, reaction time was reduced from 12 h to 30 min, Et<sub>2</sub>O was substituted for C<sub>6</sub>H<sub>6</sub> as the eluant for column chromatography.  $\text{NH}_4\text{PF}_6$ ,  $\text{NaBH}_4$ ,  $\text{NEt}_3$ , CuI and  $\text{HC}_2\text{Ph}$  were obtained commercially and used as received. Petrol refers to a mixture with boiling point range 60–80 °C. Solvents  $\text{CH}_2\text{Cl}_2$ , Et<sub>2</sub>O, MeOH, and *n*-hexane were dried using standard procedures. Thin layer chromatography (tlc) was on Merck GF<sub>254</sub> silica gel (0.5 mm); column chromatography used ungraded basic alumina.

Elemental microanalyses were performed by the Microanalysis Service Unit at the Australian National University. Infrared spectra were recorded as  $\text{CH}_2\text{Cl}_2$  solutions in  $\text{CaF}_2$  cells using a Perkin–Elmer System 2000 FT-IR. NMR spectra were recorded in  $\text{CDCl}_3$  using a Varian Gemini-300 FT NMR spectrometer and are referenced to residual solvent (<sup>1</sup>H, 300 MHz; <sup>13</sup>C, 75 MHz) or external 85%  $\text{H}_3\text{PO}_4$  (<sup>31</sup>P, 121 MHz). NMR

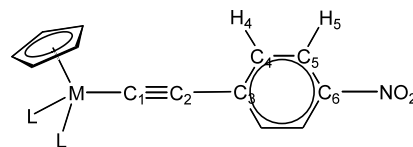


Fig. 1. NMR atom numbering scheme.

assignments follow the numbering scheme shown in Fig. 1. UV–Vis spectra were recorded using a Cary 5 spectrophotometer as thf solutions in 1 cm cells and are reported as  $\lambda_{\text{max}}$ ,  $\text{cm}^{-1}$  [ $\epsilon$ ,  $10^4 \text{ M}^{-1} \text{ cm}^{-1}$ ]. Mass spectra were recorded using a VG ZAB 2SEQ instrument (30 kV  $\text{Cs}^+$  ions, current 1 mA, accelerating potential 8 kV, 3-nitrobenzyl alcohol matrix) at the Australian National University; peaks are reported as  $m/z$  (assignment, relative intensity).

Electrochemical measurements were recorded using a MacLab 400 interface and MacLab potentiostat from ADInstruments (using a glassy carbon disc working, Pt auxiliary and Ag/AgCl reference mini-electrodes from Cypress Systems). Scan rates were typically  $100 \text{ mV s}^{-1}$ . Electrochemical solutions contained 0.1 M  $[\text{NBu}_4]^+ \text{PF}_6^-$  and approximately  $10^{-3} \text{ M}$  complex in dichloromethane. Solutions were purged and maintained under an atmosphere of nitrogen. All values are referenced to an internal sample of ferrocene (0.56 V).

Calculations were performed on a Linux-based Pentium III computer (600 MHz) using the Amsterdam Density Functional Theory (ADF) Release 1999 [22–24]. The local exchange correlation approximation of Vosko et al. [25] was used with the corrections of Becke [26] and Perdew et al. [27,28]. Triple- $\xi$  basis sets (Type IV) were used for all atoms. Core orbitals were frozen through 1s (C), 2p (P), 3p (Fe), 4p (Ru), and 4f (Os). Relativistic corrections were incorporated using the ZORA functionality [29]. Geometries were optimized using the algorithm of Versluis and Ziegler [30]. Optical spectra were calculated using the time-dependent density functional theory (TD-DFT) functionality available in ADF [31].

### 2.2. $\text{Fe}(4\text{-C}\equiv\text{CC}_6\text{H}_4\text{NO}_2)(\text{dppe})(\eta\text{-C}_5\text{H}_5)$ (**1**)

A mixture of  $\text{FeCl}(\text{dppe})(\eta\text{-C}_5\text{H}_5)$  (200 mg, 0.36 mmol), 4- $\text{HC}\equiv\text{CC}_6\text{H}_4\text{NO}_2$  and  $\text{NH}_4\text{PF}_6$  was stirred in MeOH (40 ml) for 90 min at reflux. The mixture was allowed to cool to room temperature and then 2 ml of NaOMe solution (0.33 M in MeOH) was added with stirring. The solvent was removed in vacuo and the residue was taken up in  $\text{CH}_2\text{Cl}_2$  and placed onto an alumina column. Excess acetylene was eluted using 3:7  $\text{CH}_2\text{Cl}_2$ –petrol and the product was eluted using 3:5  $\text{CH}_2\text{Cl}_2$ –petrol. The solvent was reduced to  $\sim 10 \text{ ml}$  and the resultant solid collected by filtration and washed with petrol to afford a red solid identified as **1** (75 mg, 31%). MS: 665 ( $[\text{M}]^+$ , 65), 649 ( $[\text{M}-\text{O}]^+$ , 7), 519

([Fe(dppe)(C<sub>5</sub>H<sub>5</sub>)]<sup>+</sup>, 100). Anal. Calc. for C<sub>39</sub>H<sub>33</sub>FeNO<sub>2</sub>P<sub>2</sub>: C, 70.39; H, 5.00; N, 2.10. Found: C, 70.37; H, 5.10; N, 2.30%. IR (cm<sup>-1</sup>): 2044w ν(C≡C). UV–Vis: 20 000 [1.3], 31 500 [1.0]. <sup>1</sup>H NMR: δ 2.23 (m, 2H, CH<sub>2</sub>), 2.55 (m, 2H, CH<sub>2</sub>), 4.29 (s, 5H, C<sub>5</sub>H<sub>5</sub>), 6.25 (m, 2H, H<sub>4</sub>), 7.20–7.84 (m, 22H, H<sub>5</sub>+Ph). <sup>31</sup>P NMR: δ 106.2 (s (br), PPh<sub>2</sub>).

### 2.3. Ru(4-C≡CC<sub>6</sub>H<sub>4</sub>NO<sub>2</sub>)(dppe)(η-C<sub>5</sub>H<sub>5</sub>) (2)

A mixture of RuCl(dppe)(η-C<sub>5</sub>H<sub>5</sub>) (250 mg, 0.35 mmol), 4-HC≡CC<sub>6</sub>H<sub>4</sub>NO<sub>2</sub> (130 mg, 0.88 mmol) and NH<sub>4</sub>PF<sub>6</sub> (150 mg, 0.92 mmol) was stirred in MeOH (40 ml) for 1 h at reflux. On cooling to room temperature, CH<sub>2</sub>Cl<sub>2</sub> (40 ml) was added and the mixture filtered. Addition of petrol (~20 ml) and volume reduction of the solvent in vacuo afforded a solid which was collected by filtration in air and then redissolved in CH<sub>2</sub>Cl<sub>2</sub> (10 ml). To this solution was added NaOMe solution (10 ml of a 0.1 M solution in MeOH) with stirring. The solvent was removed and the product purified by column chromatography on alumina, eluting with 65:35 CH<sub>2</sub>Cl<sub>2</sub>–petrol. Reduction of the solvent volume afforded a red solid identified as **2** (75 mg, 30%). MS: 711 ([M]<sup>+</sup>, 100), 565 ([Ru(dppe)(C<sub>5</sub>H<sub>5</sub>)]<sup>+</sup>). Anal. Calc. for C<sub>39</sub>H<sub>33</sub>NO<sub>2</sub>P<sub>2</sub>Ru: C, 65.91; H, 4.68; N, 1.97. Found: C, 65.91; H, 4.60; N, 1.79%. IR (cm<sup>-1</sup>): 2056w ν(C≡C). UV–Vis: 22 200 [1.8]. <sup>1</sup>H NMR: δ 2.30 (m, 2H, CH<sub>2</sub>), 2.57 (m, 2H, CH<sub>2</sub>), 4.79 (s, 5H, C<sub>5</sub>H<sub>5</sub>), 6.31 (d, J<sub>HH</sub> = 7 Hz, 2H, H<sub>4</sub>), 7.26–7.87 (m, 22H, H<sub>5</sub>+Ph). <sup>31</sup>P NMR: δ 86.2 (s, PPh<sub>2</sub>).

### 2.4. Os(4-C≡CC<sub>6</sub>H<sub>4</sub>NO<sub>2</sub>)(dppe)(η-C<sub>5</sub>H<sub>5</sub>) (3)

A mixture of OsBr(dppe)(η-C<sub>5</sub>H<sub>5</sub>) (160 mg, 0.22 mmol), 4-HC≡CC<sub>6</sub>H<sub>4</sub>NO<sub>2</sub> (50 mg, 0.34 mmol) and NH<sub>4</sub>PF<sub>6</sub> (75 mg, 0.46 mmol) was stirred in MeOH (30 ml) for 65 h at reflux. The solvent was removed in vacuo and the residue extracted into CH<sub>2</sub>Cl<sub>2</sub> (10 ml) and filtered through a sintered glass funnel. Et<sub>2</sub>O (50 ml) was added to the filtrate and 100 mg of yellow powder was collected. This was dissolved in CH<sub>2</sub>Cl<sub>2</sub> (10 ml) and 2 ml of NaOMe solution (0.3 M in methanol) was added with stirring. The solvent was removed and the product taken up in CH<sub>2</sub>Cl<sub>2</sub> and purified by column chromatography on alumina, eluting with CH<sub>2</sub>Cl<sub>2</sub>. The solvent was removed and the resulting dark red solid collected and identified as **3** (30 mg, 17%). MS: 802 ([M]<sup>+</sup>, 100), 655 ([Os(dppe)(C<sub>5</sub>H<sub>5</sub>)]<sup>+</sup>, 25). Anal. Calc. for C<sub>39</sub>H<sub>33</sub>NO<sub>2</sub>OsP<sub>2</sub>: C, 58.57; H, 4.16; N, 1.75. Found: C, 58.40; H, 4.11; N, 1.57%. IR (cm<sup>-1</sup>): 2055w ν(C≡C). UV–Vis: 21 600 [1.7], 36 800 (sh) [1.0]. <sup>1</sup>H NMR: δ 2.42 (m, 4H, CH<sub>2</sub>), 4.78 (s, 5H, C<sub>5</sub>H<sub>5</sub>), 6.25 (d, J<sub>HH</sub> = 9 Hz, 2H, H<sub>4</sub>), 7.17–7.38 (m, 20H, Ph), 7.72 (d, J<sub>HH</sub> = 9 Hz, 2H, H<sub>5</sub>). <sup>31</sup>P NMR: δ 46.7 (s, PPh<sub>2</sub>).

### 2.5. Os(4-C≡CC<sub>6</sub>H<sub>4</sub>NO<sub>2</sub>)(PPh<sub>3</sub>)<sub>2</sub>(η-C<sub>5</sub>H<sub>5</sub>) (4)

A mixture of OsBr(PPh<sub>3</sub>)<sub>2</sub>(η-C<sub>5</sub>H<sub>5</sub>) (250 mg, 0.29 mmol), 4-HC≡CC<sub>6</sub>H<sub>4</sub>NO<sub>2</sub> (130 mg, 0.88 mmol) and NH<sub>4</sub>PF<sub>6</sub> (150 mg, 0.92 mmol) was stirred in MeOH (40 ml) for 3 h at reflux. The mixture was allowed to cool to room temperature and then 2 ml of NaOMe solution (0.3 M in MeOH) was added with stirring. The solvent was removed and the product taken up in CH<sub>2</sub>Cl<sub>2</sub> and purified by column chromatography on alumina, eluting firstly with 3:7 CH<sub>2</sub>Cl<sub>2</sub>–petrol to remove any excess acetylene, and then with 6:4 CH<sub>2</sub>Cl<sub>2</sub>–petrol to remove the product. The solvent was removed and the product was collected to yield 210 mg (78%) of dark red microcrystals identified as **4**. MS: 927 ([M+H]<sup>+</sup>, 100), 781 ([Os(PPh<sub>3</sub>)<sub>2</sub>(C<sub>5</sub>H<sub>5</sub>)]<sup>+</sup>, 10), 664 ([M–PPh<sub>3</sub>]<sup>+</sup>, 35). Anal. Calc. for C<sub>49</sub>H<sub>39</sub>NO<sub>2</sub>OsP<sub>2</sub>: C, 63.56; H, 4.25; N, 1.51. Found: C, 63.55; H, 4.42; N, 1.61%. IR (cm<sup>-1</sup>): 2054w ν(C≡C). UV–Vis: 21 000 [2.2], 36 400 (sh) [1.6]. <sup>1</sup>H NMR: δ 4.43 (s, 5H, C<sub>5</sub>H<sub>5</sub>), 6.98 (d, J<sub>HH</sub> = 9 Hz, 2H, H<sub>4</sub>), 7.05–7.35 (m, 30H, Ph), 8.00 (d, J<sub>HH</sub> = 9 Hz, 2H, H<sub>5</sub>). <sup>31</sup>P NMR: δ 2.8 (s, PPh<sub>3</sub>).

### 2.6. Ru(4-C≡CC<sub>6</sub>H<sub>4</sub>NO<sub>2</sub>)(CO)<sub>2</sub>(η-C<sub>5</sub>H<sub>5</sub>) (5)

RuCl(CO)<sub>2</sub>(η-C<sub>5</sub>H<sub>5</sub>) (230 mg, 0.89 mmol), 4-HC≡CC<sub>6</sub>H<sub>4</sub>NO<sub>2</sub> (157 mg, 1.07 mmol) and CuI (5 mg) were stirred in NEt<sub>3</sub> (30 ml) for 2 h. The mixture was filtered and the filtrate taken to dryness. The resulting residue was taken up in CH<sub>2</sub>Cl<sub>2</sub> and subjected to tlc, eluting with 6:4 CH<sub>2</sub>Cl<sub>2</sub>–petrol. The major band was collected, taken to dryness, and the residue extracted with acetone. The solvent was removed to afford a red solid which was crystallized from Et<sub>2</sub>O–hexane to afford reddish–brown crystals of **5** (110 mg, 34%). IR (cm<sup>-1</sup>): 2108w ν(C≡C), 2056s, 2005s ν(CO). <sup>1</sup>H NMR: δ 8.03 (d, J<sub>HH</sub> = 9 Hz, 2H, H<sub>5</sub>), 7.35 (d, J<sub>HH</sub> = 9 Hz, 2H, H<sub>4</sub>), 5.45 (s, 5H, C<sub>5</sub>H<sub>5</sub>). <sup>13</sup>C NMR: δ 196.2 (CO), 144.7 (C<sub>6</sub>), 134.4 (C<sub>1</sub>), 131.9 (C<sub>4</sub>), 123.3 (C<sub>5</sub>), 110.4 (C<sub>3</sub>), 96.7 (C<sub>2</sub>), 88.0 (C<sub>5</sub>H<sub>5</sub>). Anal. Calc. for C<sub>15</sub>H<sub>9</sub>NO<sub>4</sub>Ru: C, 48.92; H, 2.46; N, 3.80. Found: C, 49.23; H, 2.23; N, 3.79%.

### 2.7. Spectroscopic data for Fe(4-C≡CC<sub>6</sub>H<sub>4</sub>NO<sub>2</sub>)(CO)<sub>2</sub>(η-C<sub>5</sub>H<sub>5</sub>) (6)

IR (cm<sup>-1</sup>): 2104m ν(C≡C), 2044s, 1999s ν(CO) cm<sup>-1</sup>. <sup>1</sup>H NMR: δ 8.03 (d, J<sub>HH</sub> = 9 Hz, 2H, H<sub>5</sub>), 7.33 (d, J<sub>HH</sub> = 9 Hz, 2H, H<sub>4</sub>), 5.06 (s, 5H, C<sub>5</sub>H<sub>5</sub>). <sup>13</sup>C NMR: δ 211.7 (CO), 144.7 (C<sub>6</sub>), 134.7 (C<sub>1</sub>), 131.5 (C<sub>4</sub>), 123.4 (C<sub>5</sub>), 116.2 (C<sub>3</sub>), 104.7 (C<sub>2</sub>), 85.5 (C<sub>5</sub>H<sub>5</sub>).

### 2.8. X-ray structural determinations

Crystals suitable for the X-ray structural analyses were grown by liquid diffusion techniques from hexane–CH<sub>2</sub>Cl<sub>2</sub> (**5**) or methanol–CH<sub>2</sub>Cl<sub>2</sub> (**2**) at 276 K. Selected

Table 1  
Crystal data and structure refinement parameters for **2** and **5**

	<b>2</b>	<b>5</b>
Empirical formula	C <sub>39</sub> H <sub>33</sub> NO <sub>2</sub> P <sub>2</sub> Ru	C <sub>15</sub> H <sub>9</sub> NO <sub>4</sub> Ru
Formula weight	710.71	368.31
Crystal size (mm)	0.16 × 0.16 × 0.06	0.36 × 0.24 × 0.18
T (K)	200	296
Wavelength (Å)	0.71069	1.5418
Crystal system	monoclinic	monoclinic
Space group	C2/c (no. 15)	P2 <sub>1</sub> /n (no. 14)
Unit cell dimensions		
<i>a</i> (Å)	29.1649(7)	15.987(3)
<i>b</i> (Å)	11.5689(3)	5.775(4)
<i>c</i> (Å)	19.7324(5)	16.054(2)
β (°)	97.389(2)	104.88(1)
<i>V</i> (Å <sup>3</sup> )	6602.5(3)	1432.5(9)
<i>Z</i>	8	4
Range for data collection, θ (°)	3.04–25.04	2.85–60.06
Index ranges	−34 ≤ <i>h</i> ≤ 34, −23 ≤ <i>l</i> ≤ 23, 0 ≤ <i>k</i> ≤ 6	−12 ≤ <i>k</i> ≤ 13, −17 ≤ <i>h</i> ≤ 0, −17 ≤ <i>l</i> ≤ 18
μ (mm <sup>−1</sup> )	6.08 (Mo Kα)	9.015 (Cu Kα)
Max./min. transmission	0.694, 0.656	0.197, 0.097
Reflections collected,	46 245	2473
<i>N</i> <sub>collected</sub>		
Independent reflections,	5834	2130
<i>N</i> <sub>unique</sub>	( <i>R</i> <sub>int</sub> = 0.060)	( <i>R</i> <sub>int</sub> = 0.081)
Observed reflections	3705	1667
( <i>I</i> > 2σ( <i>I</i> )), <i>N</i> <sub>obs</sub>		
Goodness of fit	0.70	1.66
( <i>I</i> > 2σ( <i>I</i> ))		
Final <i>R</i> indices	<i>R</i> = 0.0271,	<i>R</i> = 0.0377,
( <i>I</i> > 2σ( <i>I</i> )) <sup>a</sup>	<i>R</i> <sub>w</sub> = 0.0323	<i>R</i> <sub>w</sub> = 0.0411
<i>R</i> indices (all data) <sup>a</sup>	<i>R</i> = 0.0547,	<i>R</i> = 0.0539,
	<i>R</i> <sub>w</sub> = 0.0411	<i>R</i> <sub>w</sub> = 0.0436
<i>w</i>	[σ <sup>2</sup> ( <i>F</i> <sub>o</sub> ) + 0.00024  <i>F</i> <sub>o</sub>   <sup>2</sup> ] <sup>−1</sup>	[σ <sup>2</sup> ( <i>F</i> <sub>o</sub> ) + 0.00027  <i>F</i> <sub>o</sub>   <sup>2</sup> ] <sup>−1</sup>
Largest difference peak and hole (e Å <sup>−3</sup> )	0.26 and −0.36	0.57 and −0.52

$$^a R = \Sigma(|F_o| - |F_c|) / \Sigma F_o; \quad R_w = [\Sigma w(|F_o| - |F_c|)^2 / \Sigma w F_o^2]^{1/2}.$$

crystal data and structure refinement parameters are collected in Table 1. For each study, a single orange crystal was mounted on a glass fibre, and data were collected at 296 K on a Rigaku AFC6R diffractometer using graphite-monochromated Cu Kα radiation (**5**), or at 200 K on a Nonius KappaCCD diffractometer using graphite-monochromated Mo Kα radiation (**2**). The reduced data [32,33] were corrected for absorption using empirical ψ-scan (**5**) or numerical (**2**) [34] methods, implemented from within TEXSAN [33] and MAXUS [35], respectively. The structures were solved by direct methods [36], and expanded using difference Fourier techniques [37] within TEXSAN [33]. Non-hydrogen atoms were refined anisotropically; hydrogen atoms were included in idealized positions which were frequently recalculated. The final cycles of full-matrix

least-squares refinement were based on *N*<sub>obs</sub> observed reflections (*I* > 2σ(*I*)) and converged to *R* and *R*<sub>w</sub>. Selected bond lengths and angles for **2**, **5** and some related ruthenium alkynyl complexes are given in Table 2.

### 2.9. Hyper-Rayleigh scattering measurements

An injection seeded Nd:YAG laser (Q-switched Nd:YAG Quanta Ray GCR, 1064 nm, 8 ns pulses, 10 Hz) was focussed into a cylindrical cell (7 ml) containing the sample. The intensity of the incident beam was varied by rotation of a half-wave plate placed between crossed polarizers. Part of the laser pulse was sampled by a photodiode to measure the vertically polarized incident light intensity. The frequency doubled light was collected by an efficient condenser system and detected by a photomultiplier. The harmonic scattering and linear scattering were distinguished by appropriate filters; gated integrators were used to obtain intensities of the incident and harmonic scattered light. All measurements were performed in thf using *p*-nitroaniline (β = 21.4 × 10<sup>−30</sup> esu [50]) as a reference.

## 3. Results and discussion

### 3.1. Synthesis and characterization of metal alkynyl complexes

We have previously reported synthesis and NLO studies of (cyclopentadienyl)bis(phosphine) ruthenium alkynyl complexes [14,15,38–43], examples of which have some of the largest quadratic nonlinearities reported for organometallics; we therefore decided to investigate the effect of metal variation on β values. The syntheses of the new alkynyl metal complexes M(4-C≡CC<sub>6</sub>H<sub>4</sub>NO<sub>2</sub>)(dppe)(η-C<sub>5</sub>H<sub>5</sub>) [M = Fe (**1**), Ru (**2**), Os (**3**)] and Os(4-C≡CC<sub>6</sub>H<sub>4</sub>NO<sub>2</sub>)(PPh<sub>3</sub>)<sub>2</sub>(η-C<sub>5</sub>H<sub>5</sub>) (**4**) were based on extending published procedures for the related phenylalkynyl complexes [44], and involve the formation of an intermediate vinylidene complex by reaction of a terminal alkyne with a ligated transition metal halide, followed by deprotonation of the β-carbon of the vinylidene complex upon addition of methoxide ion (Scheme 1). For the dicarbonyl complex Ru(4-C≡CC<sub>6</sub>H<sub>4</sub>NO<sub>2</sub>)(CO)<sub>2</sub>(η-C<sub>5</sub>H<sub>5</sub>) (**5**), this route afforded only unreacted starting material. An alternate route, involving reaction of the chloro precursor and the acetylene in NEt<sub>3</sub> in the presence of catalytic amounts of CuI, was found to give the desired product (Scheme 1). The analogous iron complex, **6**, was prepared following the published route [20,45]. The new alkynyl complexes were characterized by secondary ion (SI) mass spectrometry, UV–Vis, and IR spectroscopy, <sup>1</sup>H,

Table 2  
Selected bond lengths (Å) and angles (°) for **2**, **5** and some related ruthenium alkynyl complexes

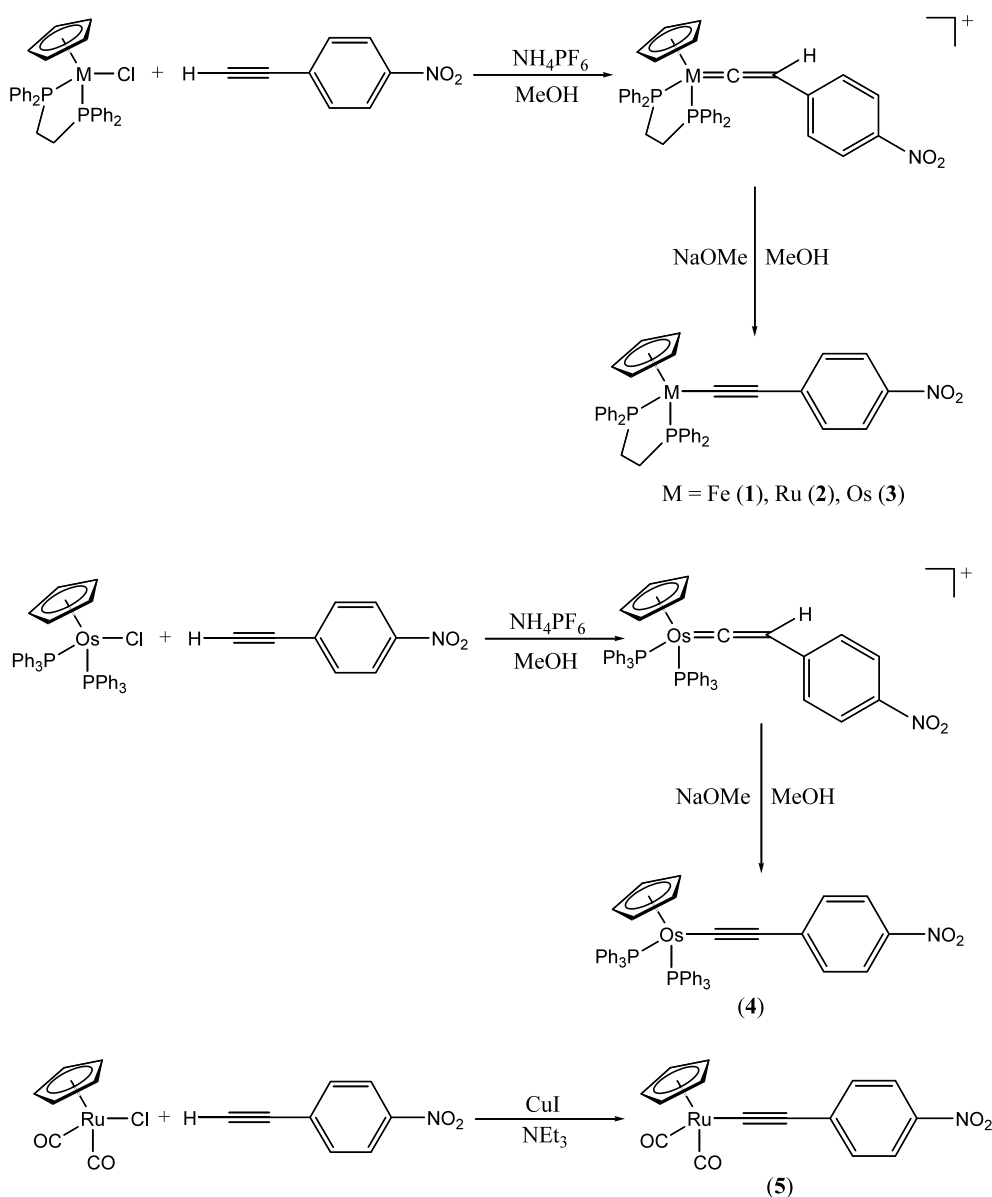
	Bond lengths			Bond angles	
	Ru(1)–C(1)	C(1)–C(2)	C(2)–C(201)	Ru–C(1)–C(2)	C(1)–C(2)–C(201)
Ru(4-C≡CC <sub>6</sub> H <sub>4</sub> NO <sub>2</sub> )(CO) <sub>2</sub> (η-C <sub>5</sub> H <sub>5</sub> ) ( <b>5</b> )	2.023(6)	1.197(9)	1.427(9)	178.9(6)	177.5(8)
Ru(4-C≡CC <sub>6</sub> H <sub>4</sub> NO <sub>2</sub> )(PMe <sub>3</sub> ) <sub>2</sub> (η-C <sub>5</sub> H <sub>5</sub> ) <sup>a</sup>	1.99(2)	1.23(2)	1.43(3)	178.0(2)	177.0(3)
Ru(4-C≡CC <sub>6</sub> H <sub>4</sub> NO <sub>2</sub> )(PPh <sub>3</sub> ) <sub>2</sub> (η-C <sub>5</sub> H <sub>5</sub> ) <sup>a</sup>	1.994(5)	1.202(8)	1.432(7)	175.9(4)	175.0(9)
Ru(4-C≡CC <sub>6</sub> H <sub>4</sub> NO <sub>2</sub> )(dppf)(η-C <sub>5</sub> H <sub>5</sub> ) ( <b>2</b> )	1.993(3)	1.214(4)	1.424(4)	177.4(3)	176.7(3)
Ru(C≡CPh)(PPh <sub>3</sub> ) <sub>2</sub> (η-C <sub>5</sub> H <sub>5</sub> ) <sup>b</sup>	2.017(5)	1.214(7)	1.462(8)	177.7(4)	170.6(5)

<sup>a</sup> Ref. [38].

<sup>b</sup> Ref. [51].

<sup>31</sup>P and, in selected cases, <sup>13</sup>C NMR spectroscopy; we have also summarized previously unreported spectroscopic data for **6**.

The SI mass spectra of the new complexes show signals due to the molecular ion, fragmentation occurring by the loss of the alkynyl ligand. The UV–Vis



Scheme 1. Syntheses of alkynyl–metal complexes.

spectra contain a band in the range 20 000–27 500  $\text{cm}^{-1}$ , tentatively assigned to the MLCT transition from the metal to the alkynyl ligand; frequencies for optical absorption maxima follow the trend  $\text{Fe} < \text{Os} < \text{Ru}$ . The IR spectra show characteristic  $\nu(\text{C}\equiv\text{C})$  bands at 2044–2056  $\text{cm}^{-1}$ , with the two iron complexes having the lowest energy bands.

### 3.2. X-ray structural studies of $\text{Ru}(4\text{-C}\equiv\text{CC}_6\text{H}_4\text{NO}_2)_2\text{L}_2(\eta\text{-C}_5\text{H}_5)$ [ $\text{L} = 1/2 \text{ dppe}$ (**2**), $\text{CO}$ (**5**)]

Structural studies of **2** and **5** were undertaken. Crystal data and structure refinement parameters are given in Table 1, and selected bond lengths and angles collected in Table 2; the latter also includes data for some related ruthenium alkynyl complexes. Figs. 2 (**2**) and 3 (**5**) contain ORTEP plots showing the molecular geometries and atomic labelling schemes.

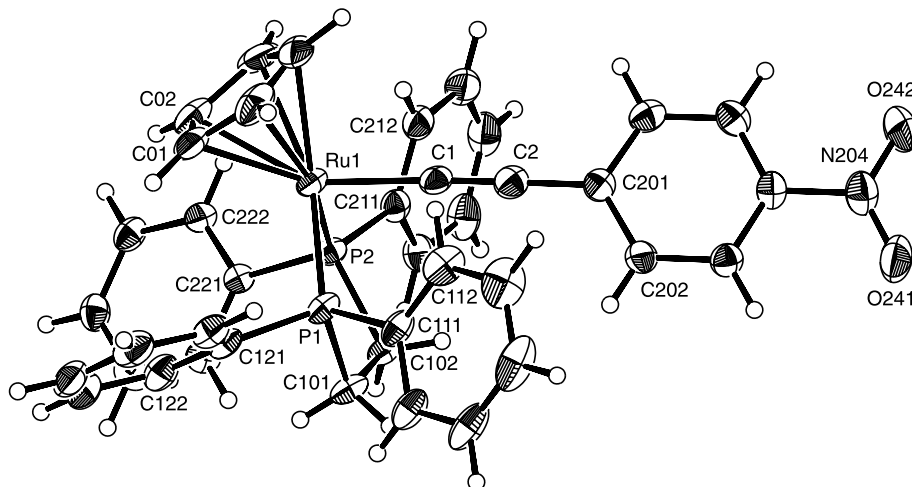


Fig. 2. Molecular structure and atom numbering scheme for  $\text{Ru}(4\text{-C}\equiv\text{CC}_6\text{H}_4\text{NO}_2)(\text{dppe})(\eta\text{-C}_5\text{H}_5)$  (**2**). 30% displacement ellipsoids are shown for non-hydrogen atoms. Hydrogen atoms have arbitrary radii.

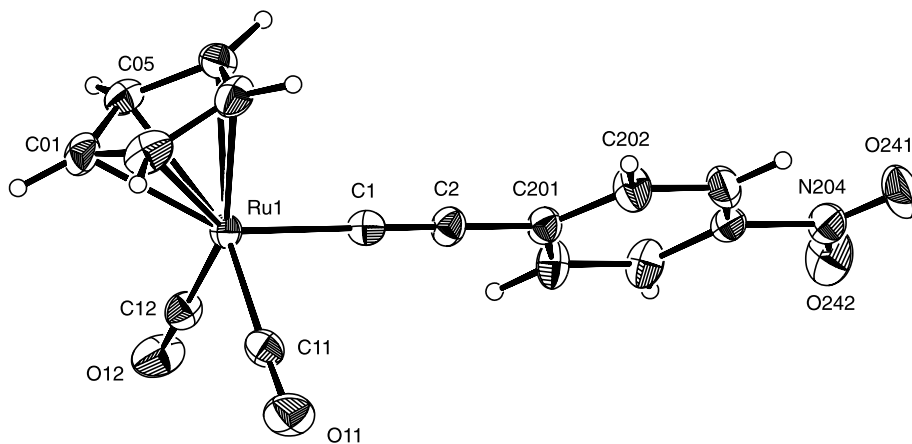


Fig. 3. Molecular structure and atom numbering scheme for  $\text{Ru}(4\text{-C}\equiv\text{CC}_6\text{H}_4\text{NO}_2)(\text{CO})_2(\eta\text{-C}_5\text{H}_5)$  (**5**). 30% displacement ellipsoids are shown for non-hydrogen atoms. Hydrogen atoms have arbitrary radii.

The structural data in Table 2 provide the opportunity to assess the effect of systematic structural modifications on important metrical parameters. However, most differences which exist are not statistically significant. Thus, the  $\text{Ru}(1)\text{-C}(1)$  distance decreases on proceeding from **5** to **2** and  $\text{Ru}(4\text{-C}\equiv\text{CC}_6\text{H}_4\text{NO}_2)(\text{PPh}_3)_2(\eta\text{-C}_5\text{H}_5)$ , consistent with greater  $\pi$ -backbonding to the alkynyl ligand from the more electron-rich metal centers in the latter complexes, but other variations in bond distances are not meaningful. The small deviations in bond angles  $\text{Ru-C}(1)\text{-C}(2)$  and  $\text{C}(1)\text{-C}(2)\text{-C}(201)$  from the idealized  $180^\circ$  probably reflect crystal packing effects.

### 3.3. Electrochemical studies

Cyclic voltammetric data are summarized in Table 3. Complexes **1**, **2**, **4**, **5**, and **7** exhibit anodic and cathodic processes assigned to metal-centered oxidation and

Table 3  
Cyclic voltammetric data

Compound	$E_{1/2}$ (V) [ $i_{pc}/i_{pa}$ ] $M^{II/III}$ (V)	$E_{1/2}$ [ $i_{pa}/i_{pc}$ ] $NO_2^{0/-1}$ (V)
Fe(4-C≡CC <sub>6</sub> H <sub>4</sub> NO <sub>2</sub> )(CO) <sub>2</sub> - (η-C <sub>5</sub> H <sub>5</sub> ) ( <b>6</b> )	<sup>a</sup>	-1.04 [0.7]
Ru(4-C≡CC <sub>6</sub> H <sub>4</sub> NO <sub>2</sub> )(CO) <sub>2</sub> - (η-C <sub>5</sub> H <sub>5</sub> ) ( <b>5</b> )	0.86 [0.7]	-1.07 [0.8]
Fe(4-C≡CC <sub>6</sub> H <sub>4</sub> NO <sub>2</sub> )(dppe)- (η-C <sub>5</sub> H <sub>5</sub> ) ( <b>1</b> )	0.29 [0.6]	-1.13 [0.7]
Ru(4-C≡CC <sub>6</sub> H <sub>4</sub> NO <sub>2</sub> )(dppe)- (η-C <sub>5</sub> H <sub>5</sub> ) ( <b>2</b> )	0.67 [0.9]	-0.93 [1]
Ru(4-C≡CC <sub>6</sub> H <sub>4</sub> NO <sub>2</sub> )(PPh <sub>3</sub> ) <sub>2</sub> - (η-C <sub>5</sub> H <sub>5</sub> ) ( <b>7</b> ) <sup>b</sup>	0.73 [1]	-1.08 [1]
Os(4-C≡CC <sub>6</sub> H <sub>4</sub> NO <sub>2</sub> )(PPh <sub>3</sub> ) <sub>2</sub> - (η-C <sub>5</sub> H <sub>5</sub> ) ( <b>4</b> )	0.59 [1]	-1.17 [0.5]

Ag/AgCl reference electrode (FcH/FcH<sup>+</sup> 0.56 V). See Ref. [46].

<sup>a</sup> No oxidation process observed to switching potential of 1.2 V.

<sup>b</sup> Ref. [15].

nitro-centered reduction, respectively. Reversibility of the metal-centered oxidation increases on replacing Fe by Ru (proceeding from **1** to **2**) and replacing co-ligand CO by dppe (proceeding from **5** to **2**); complexes **4** and **7** are the only examples in this system with reversible metal-centered oxidation. Ease of oxidation increases on replacing Ru by Os (on proceeding from **7** to **4**) or Fe (on proceeding from **2** to **1**), consistent with the trend in optical absorption maxima, for which  $\lambda_{max}$  increases on replacing Ru by Os or Fe.

### 3.4. Nonlinear optical studies

The results of hyper-Rayleigh scattering (HRS) experiments are presented in Table 4, together with the data we recently obtained for a series of related complexes **8–10** containing 1,2-bis(methylphenylphosphino)benzene (diph) ligands [46]. The experimental

first hyperpolarizabilities ( $\beta_{HRS}$ ) are shown together with static first hyperpolarizabilities ( $\beta_0$ ) calculated from the experimental values using the two-level approximation [the shortcomings of the two-level model have been discussed elsewhere (e.g., Ref. [2]). This model was developed for a restricted class of organic compounds where structural modifications are directed at the charge-transfer band thought to contribute to the hyperpolarizability, and may not be useful where there are several dominant transitions close to  $2\omega$ ].

A comparison of the  $\beta_{HRS}$  values indicates that the iron-containing complexes have similar or lower responses than ruthenium-containing analogues, in contrast to the trend reported for donor–acceptor nitrile [11] and metallocenyl complexes [7–10] for which the relative efficiency Fe > Ru was found. In the current work, the iron acetylide complexes have absorption bands closer to the second-harmonic wavelength of 532 nm than either the ruthenium or osmium analogues, suggesting that the  $\beta_{HRS}$  values for the iron complexes contain a larger resonance contribution. The  $\beta_{HRS}$  values for the osmium acetylide complexes are in each case greater than the values for the ruthenium-containing complexes. Absorption bands for the osmium complexes are closer to the second harmonic than are those of their ruthenium homologues. For the cyclopentadienyl complexes, calculating static  $\beta$  values from the experimental  $\beta_{HRS}$  values using a two-level model affords the same trend as for the experimental values, except that  $\beta_0$  (**1**) <  $\beta_0$  (**2**). The ruthenium complex has the highest calculated static value for complexes **8–10**. While this suggests some ambiguity, the two-level model may have limited applicability with organometallic complexes of this type (see above). Despite experimental uncertainties ( $\pm 10\%$  in reported values) there is sufficient data to suggest that  $\beta_{HRS}$  values for alkynyl complexes of this type follow the ordering: iron ≤

Table 4  
Linear optical and quadratic NLO response parameters<sup>a</sup>

Compound	$\lambda_{max}$ (nm) [ $\epsilon$ ( $10^4$ M <sup>-1</sup> cm <sup>-1</sup> )]	$\beta_{HRS}$ <sup>b</sup> ( $10^{-30}$ esu)	$\beta_0$ <sup>c</sup> ( $10^{-30}$ esu)
Fe(4-C≡CC <sub>6</sub> H <sub>4</sub> NO <sub>2</sub> )(CO) <sub>2</sub> (η-C <sub>5</sub> H <sub>5</sub> ) ( <b>6</b> )	370 [1.3]	49	22
Ru(4-C≡CC <sub>6</sub> H <sub>4</sub> NO <sub>2</sub> )(CO) <sub>2</sub> (η-C <sub>5</sub> H <sub>5</sub> ) ( <b>5</b> )	364 [1.6]	58	27
Fe(4-C≡CC <sub>6</sub> H <sub>4</sub> NO <sub>2</sub> )(dppe)(η-C <sub>5</sub> H <sub>5</sub> ) ( <b>1</b> )	498 [1.3]	665	64
Ru(4-C≡CC <sub>6</sub> H <sub>4</sub> NO <sub>2</sub> )(dppe)(η-C <sub>5</sub> H <sub>5</sub> ) ( <b>2</b> )	447 [1.8]	664	161
Os(4-C≡CC <sub>6</sub> H <sub>4</sub> NO <sub>2</sub> )(dppe)(η-C <sub>5</sub> H <sub>5</sub> ) ( <b>3</b> )	461 [1.7]	929	188
(-) <sub>436</sub> -trans-Fe(4-C≡CC <sub>6</sub> H <sub>4</sub> NO <sub>2</sub> )Cl{(R,R)-diph} <sub>2</sub> ( <b>8</b> ) <sup>d</sup>	543 [1.7]	440	-14
(-) <sub>589</sub> -trans-Ru(4-C≡CC <sub>6</sub> H <sub>4</sub> NO <sub>2</sub> )Cl{(R,R)-diph} <sub>2</sub> ( <b>9</b> ) <sup>d</sup>	467 [2.1]	528	97
(-) <sub>365</sub> -trans-Os(4-C≡CC <sub>6</sub> H <sub>4</sub> NO <sub>2</sub> )Cl{(R,R)-diph} <sub>2</sub> ( <b>10</b> ) <sup>d</sup>	490 [1.8]	620	74
Ru(4-C≡CC <sub>6</sub> H <sub>4</sub> NO <sub>2</sub> )(PPh <sub>3</sub> ) <sub>2</sub> (η-C <sub>5</sub> H <sub>5</sub> ) ( <b>7</b> )	460 [1.1]	468	96
Os(4-C≡CC <sub>6</sub> H <sub>4</sub> NO <sub>2</sub> )(PPh <sub>3</sub> ) <sub>2</sub> (η-C <sub>5</sub> H <sub>5</sub> ) ( <b>4</b> )	474 [2.2]	1051	174

<sup>a</sup> All compounds are optically transparent at the fundamental frequencies. All measurements in solvent thf.

<sup>b</sup> HRS at 1064 nm; values  $\pm 10\%$ , using *p*-nitroaniline ( $\beta = 21.4 \times 10^{-30}$  esu) as a reference.

<sup>c</sup> Data corrected for resonance enhancement at 532 nm using the two-level model with  $\beta_0 = \beta [1 - (2\lambda_{max}/1064)^2] [1 - (\lambda_{max}/1064)^2]$ ; damping factors not included.

<sup>d</sup> Ref [46]; diph = 1,2-bis(methylphenylphosphino)benzene.

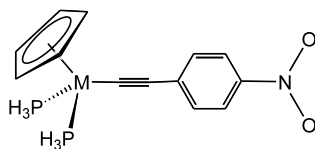


Fig. 4. Molecular geometry used to calculate optical transitions.

ruthenium  $\leq$  osmium, contrary to previously reported trends for other organometallics.

Comparison of the  $\beta_{\text{HRS}}$  values for **1**, **2**, **5**, and **6** permits comment on the effect of varying co-ligands. Replacement of the electron-donating diphosphine ligand with the relatively strongly electron-withdrawing carbonyls results in a significant reduction of the second-order NLO response. This is readily rationalized as the amount of electron density available to the donating metal center (and hence its donor strength) being reduced on replacing diphosphine by two carbonyl groups. Ligated metals are, therefore, efficient *tunable* donors in alkyne complexes.

### 3.5. Calculations

TD-DFT was employed to investigate the optical spectra, and the bonding between the acetylide ligand and the metal fragment, in order to shed light on the observed trend in optical nonlinearities. The model complexes  $\text{M}(4\text{-C}\equiv\text{CC}_6\text{H}_4\text{NO}_2)(\text{PH}_3)_2(\eta\text{-C}_5\text{H}_5)$  (Fig. 4) were used in calculations to approximate the complexes  $\text{M}(4\text{-C}\equiv\text{CC}_6\text{H}_4\text{NO}_2)(\text{dppe})(\eta\text{-C}_5\text{H}_5)$  (for which the complete set  $\text{M} = \text{Fe}, \text{Ru}, \text{Os}$  exists, and which were examined experimentally in the present study). The calculated optical transitions show good correlation with the experimental results (Table 5); differences between the calculated and observed MLCT and phenyl  $\rightarrow$  phenyl\* transitions are small, considering the approximations used to generate the calculated spectra (phosphine replacement, isolated molecules in the gas phase c.f. experimental data obtained in solution). A molecular orbital diagram of one example, namely  $\text{Fe}(4\text{-C}\equiv\text{CC}_6\text{H}_4\text{NO}_2)(\text{PH}_3)_2(\eta\text{-C}_5\text{H}_5)$ , is shown in Fig. 5. We have previously described the electronic structure of

$\text{Ru}(\text{C}\equiv\text{CH})(\text{PH}_3)_2(\eta\text{-C}_5\text{H}_5)$  [47]; the present study extends this investigation to other Group 8 metals and a strongly electron-withdrawing alkyne ligand. The square-pyramidal  $\text{M}(\text{PH}_3)_2(\eta\text{-C}_5\text{H}_5)$  fragment (in which the  $\eta\text{-C}_5\text{H}_5$  ligand occupies three facially disposed coordination sites) and the planar  $4\text{-C}\equiv\text{CC}_6\text{H}_4\text{NO}_2$  ligand interact strongly via overlap of the singly occupied  $15a'$  orbital of the former (essentially  $d_{z^2}$  in character) with the singly occupied  $18a'$  orbital of the latter (an sp-hybridized  $\sigma$ -orbital). For the  $\text{M}(\text{PH}_3)_2(\eta\text{-C}_5\text{H}_5)$  unit,  $13a'$  and  $11a''$  (essentially  $d_{xy}$  and  $d_{x^2-y^2}$  in character, respectively) are non-bonding, transforming to  $34a'$  and  $18a''$  in the alkyne complex. Orbitals  $14a'$  and  $10a''$  of the ligated metal unit (comprised, principally, of  $d_{xz}$  and  $d_{yz}$  contributions) have  $\pi$  symmetry with respect to the alkyne–metal axis, and interact with filled arylalkynyl  $\pi$  orbitals ( $3a''$ ,  $19a'$ ,  $6a''$ ) in a destabilizing manner and with vacant  $\pi$  orbitals ( $7a''$ ,  $9a''$ ,  $22a'$ ,  $10a''$ ) in a stabilizing manner. The transitions in the optical spectra summarized in Table 5 correspond to  $16a'' \rightarrow 17a''$  (MLCT) and  $15a'' \rightarrow 17a''$  (phenyl  $\rightarrow$  phenyl\*).

## 4. Discussion

Correlating readily accessible spectroscopic or electrochemical parameters with NLO properties would, if successful, afford information about the NLO responses of complexes without recourse to less readily available NLO measurements. While connections between linear optical properties and NLO properties have been probed significantly [48], the present studies suggest that relationships between other physical data (e.g., redox potentials and NMR resonances) and quadratic hyperpolarizability should be made with caution. Garcia and co-workers [11] established a correlation between  $\nu(\text{N}\equiv\text{C})$  and  $\beta_{\text{HRS}}$  for the nitrile complex cations  $[\text{M}(\text{N}\equiv\text{CC}_6\text{H}_4\text{-4-R})(\text{dppe})(\eta\text{-C}_5\text{H}_5)]^+$  ( $\text{M} = \text{Fe}, \text{Ru}$ ;  $\text{R} = \text{Ph}, \text{NMe}_2, \text{NO}_2, \text{C}_6\text{H}_4\text{NO}_2$ ), for which lower energy IR bands correspond to larger optical nonlinearities. This correspondence can be rationalized if  $\nu(\text{N}\equiv\text{C})$  is indica-

Table 5  
Observed and calculated optical transitions

	$\nu_{\text{max}}$ ( $\text{cm}^{-1}$ ) ( $\epsilon$ , $\text{M}^{-1} \text{cm}^{-1}$ ) (Expt.) <sup>a</sup>	$\nu_{\text{max}}$ ( $\text{cm}^{-1}$ ) ( $f$ ) (Calc.) <sup>b</sup>	Transition
$\text{Fe}(4\text{-C}\equiv\text{CC}_6\text{H}_4\text{NO}_2)(\text{PH}_3)_2(\eta\text{-C}_5\text{H}_5)$	20 000 (13 000) 31 490 (9800)	18 000 (0.36) 28 700 (0.25)	MLCT phenyl $\rightarrow$ phenyl*
$\text{Ru}(4\text{-C}\equiv\text{CC}_6\text{H}_4\text{NO}_2)(\text{PH}_3)_2(\eta\text{-C}_5\text{H}_5)$	22 200 (18 000) 33 700 (8800)	19 000 (0.45) 32 400 (0.18)	MLCT phenyl $\rightarrow$ phenyl*
$\text{Os}(4\text{-C}\equiv\text{CC}_6\text{H}_4\text{NO}_2)(\text{PH}_3)_2(\eta\text{-C}_5\text{H}_5)$	21 600 (17 000) 36 800 (10 400)	20 100 (0.49) 30 800 (0.18)	MLCT phenyl $\rightarrow$ phenyl*

<sup>a</sup> Experimental results are taken from  $\text{M}(4\text{-C}\equiv\text{CC}_6\text{H}_4\text{NO}_2)(\text{dppe})(\eta\text{-C}_5\text{H}_5)$ .

<sup>b</sup> All other calculated transitions are at least two orders of magnitude lower in oscillator strength.

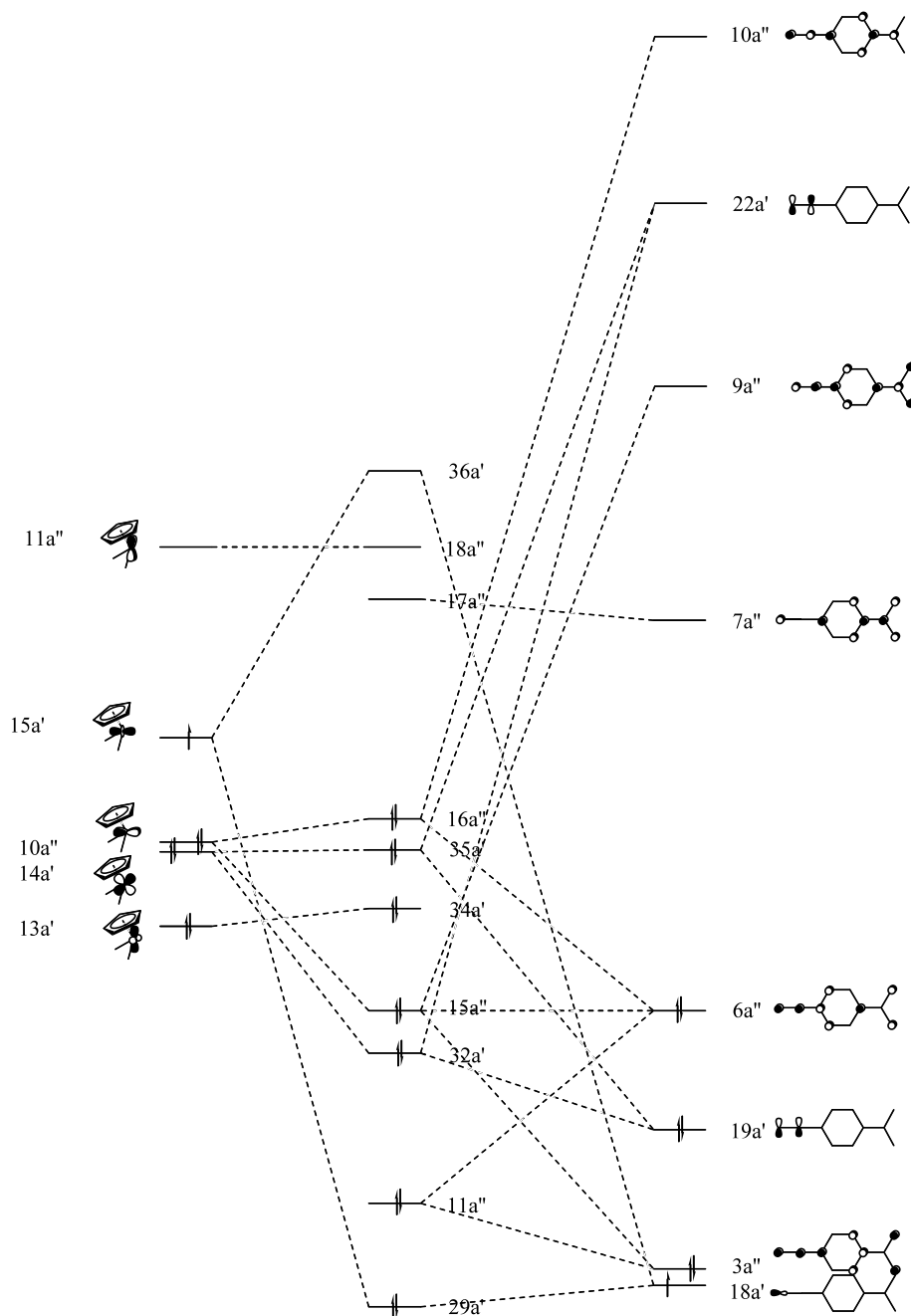


Fig. 5. Molecular orbital diagram of  $\text{Fe}(4\text{-C}\equiv\text{CC}_6\text{H}_4\text{NO}_2)(\text{PH}_3)_2(\eta\text{-C}_5\text{H}_5)$ . Noninteracting orbitals have been removed for clarity.

tive of the extent of  $\pi$ -backbonding, and if  $\pi$ -backbonding is an important determinant of NLO merit. No similar correspondence between  $\nu(\text{C}\equiv\text{C})$  and quadratic nonlinearity is seen with the present series of complexes. It is probable, though, that  $\nu(\text{C}\equiv\text{C})$  is not a useful determinant of backbonding, because stretching vibrations are frequently coupled. We have recently assessed  $\pi$ -backbonding in the complexes  $\text{trans-M}(\text{C}\equiv\text{CR})\text{Cl}(\text{PH}_3)_4$  ( $\text{M} = \text{Fe}, \text{Ru}, \text{Os}$ ;  $\text{R} = \text{H}, \text{Ph}, 4\text{-C}_6\text{H}_4\text{NO}_2$ ) using DFT, for which  $\text{M}-\text{C}$  bond energy varies as  $\text{Fe} < \text{Ru} < \text{Os}$  when relativistic terms are included [49]. This is not unexpected; the relevant  $d_{\pi}$

orbitals of osmium should be significantly higher in energy than those of iron, resulting in a stronger interaction with the alkynyl ligand  $\pi^*$  orbitals, and hence stronger  $\pi$ -backbonding. The present work confirms this ordering in the cyclopentadienyl system, establishes the transition which is the most important contributor to optical nonlinearity as clearly MLCT in character, and reproduces the trend in absorption maxima. The calculations suggest that  $\pi$ -backbonding is important for NLO merit, but that correlations with easily accessible spectroscopic or electrochemical parameters should be made with caution.

## 5. Supplementary material

Crystallographic data for the structural analysis have been deposited with the Cambridge Crystallographic Data Centre, CCDC Nos. 168645 (5), 169737 (2). Copies of this information may be obtained free of charge from The Director, CCDC, 12 Union Road, Cambridge, CB2 1E2, UK (fax: +44-1223-336-033; email: deposit@ccdc.cam.ac.uk, www: <http://www.ccdc.cam.ac.uk>).

## Acknowledgements

We thank the Australian Research Council (MGH), the Fund for Scientific Research, Flanders (G.0338.98, G.0407.98) (AP), the Belgian Government (IUAP-IV/11) (AP) and the K.U. Leuven (GOA/2000/03) (AP) for support of this work, and Johnson–Matthey Technology Centre (MGH) for the generous loan of ruthenium and osmium salts. MGH holds an ARC Australian Senior Research Fellowship.

## References

- [1] S.K. Hurst, N.T. Lucas, M.G. Humphrey, I. Asselberghs, A. Persoons, *Aust. J. Chem.*, 54 (2001) 447.
- [2] I.R. Whittall, A.M. McDonagh, M.G. Humphrey, M. Samoc, *Adv. Organomet. Chem.* 42 (1998) 291.
- [3] I.R. Whittall, A.M. McDonagh, M.G. Humphrey, M. Samoc, *Adv. Organomet. Chem.* 43 (1999) 349.
- [4] N.J. Long, *Angew. Chem., Int. Ed. Engl.* 34 (1995) 21.
- [5] T. Verbiest, S. Houbrechts, M. Kauranen, K. Clays, A. Persoons, *J. Mater. Chem.* 7 (1997) 2175.
- [6] S.R. Marder, in: D.W. Bruce, D. O'Hare (Eds.), *Inorganic Materials*, Wiley, New York, 1992.
- [7] S.R. Marder, B.G. Tiemann, J.W. Perry, L.T. Cheng, W. Tam, W.P. Schaefer, R.E. Marsh, in: S.R. Marder, G.D. Stucky, J.E. Simon, *Materials for Nonlinear Optics*, ACS Symp. Ser. 455, 1991 ACS, New York, p. 187.
- [8] J.C. Calabrese, L.-T. Cheng, J.C. Green, S.R. Marder, W. Tam, *J. Am. Chem. Soc.* 113 (1991) 7227.
- [9] L.T. Cheng, W. Tam, G.R. Meredith, S.R. Marder, *Mol. Cryst. Liq. Cryst.* 189 (1990) 137.
- [10] S.R. Marder, D.N. Beratan, B.G. Tiemann, L.T. Cheng, W. Tam, *Org. Mater. Nonlinear Opt., Spec. Publ. R. Soc. Chem.* 91 (1991) 165.
- [11] W. Wenseleers, A.W. Gerbrandij, E. Goovaerts, M.H. Garcia, M.P. Robalo, P.J. Mendes, J.C. Rodrigues, A.R. Dias, *J. Mater. Chem.* 8 (1998) 925.
- [12] I.R. Whittall, M.G. Humphrey, S. Houbrechts, A. Persoons, D.C.R. Hockless, *Organometallics* 15 (1996) 5738.
- [13] I.R. Whittall, M.P. Cifuentes, M.G. Humphrey, B. Luther-Davies, M. Samoc, S. Houbrechts, A. Persoons, G.A. Heath, D. Bogsanyi, *Organometallics* 16 (1997) 2631.
- [14] I.R. Whittall, M.G. Humphrey, A. Persoons, S. Houbrechts, *Organometallics* 15 (1996) 1935.
- [15] I.R. Whittall, M.P. Cifuentes, M.G. Humphrey, B. Luther-Davies, M. Samoc, S. Houbrechts, A. Persoons, G.A. Heath, D.C.R. Hockless, *J. Organomet. Chem.* 549 (1997) 127.
- [16] S. Takahashi, Y. Kuroyama, K. Sonogashira, N. Hagihara, *Synthesis* (1980) 627.
- [17] A. Eisenstadt, R. Tannenbaum, A. Efraty, *J. Organomet. Chem.* 221 (1981) 317.
- [18] R.B. King, L.W. Houk, K.H. Pannell, *Inorg. Chem.* 8 (1969) 1042.
- [19] G.S. Ashby, M.I. Bruce, I.B. Tompkins, R.C. Wallis, *Aust. J. Chem.* 32 (1979) 1003.
- [20] H. Fischer, F. Leroux, G. Roth, R. Stumpf, *Organometallics* 15 (1996) 3723.
- [21] G. Jia, W.S. Ng, J. Yao, C.P. Lau, Y. Chen, *Organometallics* 15 (1996) 5039.
- [22] E.J. Baerends, D.E. Ellis, P. Ros, *Chem. Phys.* 2 (1973) 42.
- [23] E.J. Baerends, P. Ros, *Chem. Phys.* 2 (1973) 52.
- [24] E.J. Baerends, P. Ros, *Int. J. Quantum Chem. S12* (1978) 169.
- [25] S.H. Vosko, L. Wilk, M. Nusair, *Can. J. Phys.* 58 (1980) 1200.
- [26] A.D.J. Becke, *Chem. Phys.* 84 (1986) 4524.
- [27] J.P. Perdew, J.A. Chevary, S.H. Vosko, K.A. Jackson, M.R. Pederson, D.J. Singh, C. Fiolhais, *Phys. Rev. A* 46 (1992) 6671.
- [28] J.P. Perdew, *Phys. Rev. B* 33 (1986) 8822.
- [29] E. van Lenthe, E.J. Baerends, J.G.J. Snijders, *Chem. Phys.* 99 (1993) 4597.
- [30] L. Versluis, T. Ziegler, *J. Chem. Phys.* 88 (1988) 322.
- [31] S.J.A. van Gisbergen, J.G. Snijders, E.J. Baerends, *Comput. Phys. Commun.* 118 (1999) 119.
- [32] Z. Otwinowski, W. Minor (Eds.), *Methods in Enzymology*, Academic Press, New York, 1997, p. 307.
- [33] TEXSAN, Single Crystal Structure Analysis Software, Version 1.8, Molecular Structure Corporation, The Woodlands, TX, 1996.
- [34] P. Coppens (Ed.), *Crystallographic Computing*, Munksgaard, Copenhagen, 1970, p. 255.
- [35] S. Mackay, C.J. Gilmore, C. Edwards, M. Tremayne, N. Stuart, K. Shankland, MAXUS Computer Program for the Solution, Refinement of Crystal Structures, Nonius, Delft, MacScience, Japan, The University of Glasgow, 2000.
- [36] A. Altomare, M. Cascarano, C. Giacovazzo, A. Guagliardi, M.C. Burla, G. Polidori, M. Camalli, *J. Appl. Cryst.* 27 (1994) 425.
- [37] P.T. Beurskens, G. Admiraal, W.P. Bosman, S. Garcia-Granda, R.O. Gould, J.M.M. Smits, C. Smykalla, *The DIRDIF Program System*. Technical Report of the Crystallographic Laboratory, University of Nijmegen, Nijmegen, The Netherlands, 1994.
- [38] I.R. Whittall, M.G. Humphrey, D.C.R. Hockless, B.W. Skelton, A.H. White, *Organometallics* 14 (1995) 3970.
- [39] I.R. Whittall, M.G. Humphrey, M. Samoc, J. Swiatkiewicz, B. Luther-Davies, *Organometallics* 14 (1995) 5493.
- [40] R.H. Naulty, M.P. Cifuentes, M.G. Humphrey, S. Houbrechts, C. Boutton, A. Persoons, G.A. Heath, D.C.R. Hockless, B. Luther-Davies, M. Samoc, *J. Chem. Soc., Dalton Trans.* (1997) 4167.
- [41] A.M. McDonagh, M.P. Cifuentes, N.T. Lucas, M.G. Humphrey, S. Houbrechts, A. Persoons, *J. Organomet. Chem.* 605 (2000) 193.
- [42] A.M. McDonagh, N.T. Lucas, M.P. Cifuentes, M.G. Humphrey, S. Houbrechts, A. Persoons, *J. Organomet. Chem.* 605 (2000) 184.
- [43] S. Hurst, N.T. Lucas, M.P. Cifuentes, M.G. Humphrey, M. Samoc, B. Luther-Davies, I. Asselberghs, R. Van Boxel, A. Persoons, *J. Organomet. Chem.* 633 (2001) 114.
- [44] M.I. Bruce, R.C. Wallis, *Aust. J. Chem.* 32 (1979) 1471.
- [45] M.P. Gamasa, J. Gimeno, E. Lastra, M. Lanfranchi, A. Tiripicchio, *J. Organomet. Chem.* 405 (1991) 333.
- [46] A.M. McDonagh, M.P. Cifuentes, M.G. Humphrey, S. Houbrechts, A. Persoons, *J. Organomet. Chem.* 610 (2000) 71.
- [47] J.E. McGrady, T. Lovell, R. Stranger, M.G. Humphrey, *Organometallics* 16 (1997) 4004.
- [48] D.R. Kanis, M.A. Ratner, T.J. Marks, *Chem. Rev.* 94 (1994) 195.
- [49] C.D. Delfs, R. Stranger, M.G. Humphrey, A.M. McDonagh, *J. Organomet. Chem.* 607 (2000) 208.
- [50] M. Stähelin, D.M. Burland, J.E. Rice, *Chem. Phys. Lett.* 191 (1992) 245.
- [51] M.I. Bruce, M.G. Humphrey, M.R. Snow, E.R.T. Tiekink, *J. Organomet. Chem.* 314 (1986) 213.